 DOI: 10.1002/maco.200804104

Kinetics of corrosion inhibition of benzotriazole to copper in 3.5% NaCl

F. M. Bayoumi*, **A. M. Abdullah and B. Attia**

The kinetics of interaction of benzotriazole (BTAH) with the surface of copper were studied using an electrochemical quartz crystal microbalance (EQMB) and electrochemical impedance spectroscopy (EIS). Upon injecting BTAH into the electrolyte, three regions appear in the time response of the microbalance. Region I (at short time scale of few minutes) exhibits rapid linear growth of mass with time. This is attributed to the formation of a Cu(I)BTA film that is several hundred layers thick. Region II reveals adsorption of BTAH at a slower rate, on the inner Cu(I)BTA complex. Region III is a plateau indicating that the BTAH film attains an equilibrium thickness, which increases with the concentration of BTAH. The polarization resistance of the interface changes with time in a similar fashion while the double layer capacitance decreases. The results suggest that the thickness of the physically adsorbed film of BTAH increases with time and BTAH concentration while the thickness of the inner Cu(I)BTA remains constant. Two semicircles were obtained in the impedance spectra corresponding to the complex Cu(I)BTA and the physically adsorbed BTAH.

1 Introduction

Benzotriazole ($C_6H_5N_3$, BTAH) has been extensively studied as an inhibitor for the corrosion of copper and many of its alloys [1–16], for dezincification of brass [17,18], and as an additive in the etching [19], electrodeposition [20–22], and in the chemical mechanical polishing of copper [23–25]. It has also been reported to inhibit the corrosion of iron [26–28], cobalt [29], zinc [30], and nickel [28] and to enhance the resistance of tin bronze to oxidation in air up to 500 °C [31]. The remarkable inhibiting efficiency of BTAH is attributed to adsorption [32,34] and complex formation [34–38], i.e.,

$$\mathrm{BTAH} + \mathrm{Cu} = \mathrm{BTAH{:}Cu} \quad (1)$$

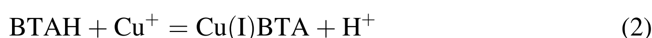

$$\mathrm{BTAH} + \mathrm{Cu}^{+} = \mathrm{Cu(I)BTA} + \mathrm{H}^{+} \quad (2)$$

where BTAH:Cu refers to adsorbed BTAH and Cu(I)BTA is a polymeric complex.

Most of the previous studies were concerned with the inhibiting efficiency and characterization of the films that have been grown on the metallic surface after sufficiently long times. The kinetics of interaction of BTAH with the surface of copper have not attracted much attention. This is believed to be due to the complexity of the kinetic behavior and also the difficulty of performing such measurements.

It is now possible to follow such a behavior in situ and in real time using an electrochemical quartz crystal microbalance (EQMB). This balance utilizes the piezoelectric properties of quartz crystals [39]. Crystals which acquire a charge when compressed, twisted, or distorted are said to be piezoelectric. A quartz crystal has a well-defined natural frequency, f (caused by its shape and size) at which it prefers to oscillate. Loss or gain of mass from the surface of the crystal changes the frequency f. The change in mass (Δm) and in the oscillation frequency (Δf) are related by the following equation [40,41]:

$$\Delta f = -2\Delta m f^2 / A(\mu \rho_q)^{1/2} = -C_f \Delta m \quad (3)$$

where f is the oscillation frequency of the quartz crystal (9 MHz), Δm the elastic mass change (g), A the electrode area (0.196 cm^2), ρ_q the density of quartz (2.648 g/cm^3), and μ is the shear modulus of the crystal (2.947×10^{11} $g/cm/s^2$). The constant C_f is the integrated EQMB sensitivity, which has a value of 0.9363 Hz/ng. This equation can then be simplified to

$$\Delta m = -1.068\ \Delta f \quad (4)$$

where Δm is in nanograms and f is in Hertz. Equation (4) is valid for small evenly distributed elastic masses added to or taken from the crystal surface and when the mass change is within 2% of the mass of the quartz crystal [39,40]. Many factors affect the accuracy of measurements of the EQMB such as surface roughness, density, and viscosity of the liquid in contact with the crystal [41]. The EQMB has been used in studies of corrosion and protection of metals [13–15,42–49].

The objective of this paper is to analyze the kinetics of interaction of BTAH with the surface of copper in salt water. This is pursued using an EQMB and electrochemical impedance spectroscopy. This approach enables one to follow the kinetics of the process in situ and in real time.

2 Experimental

The quartz crystal used in these experiments is an AT-cut disk of area 0.196 cm^2 (diameter 2.5 mm) and its nominal

* *F. M. Bayoumi, A. M. Abdullah, B. Attia*
Faculty of Science, University of Kuwait, Khalideya, Kuwait City (Kuwait)

F. M. Bayoumi
Present address: Central Metallurgical R & D Institute, P.O. Box: 87 Helwan, Cairo (Egypt)
E-mail: fm0159@yahoo.com

 © 2008 WILEY-VCH Verlag GmbH & Co. KGaA, Weinheim

WILEY InterScience® DISCOVER SOMETHING GREAT

resonant frequency is 9 MHz. On both sides, a 3000 Å thick layer of Au was sputtered on a 100 Å Ti. The crystal holder is a well-type shaped holder (QA-CL4) which was obtained from Seiko EG&G Co., Ltd. The EQMB (QCM922 from Seiko EG&G Co., Ltd.) was coupled with a Gamry PCI4 Potentiostat. A conventional three-electrode cell was used with a Ag/AgCl reference electrode, $E = 0.197$ V SHE, and a Pt sheet counter electrode. All measurements were performed in 3.5% NaCl under free corrosion conditions. Copper was electroplated from an acid sulfate bath and inspected microscopically to ensure a uniform layer. The copper-coated quartz crystal was immersed in the electrolyte for 1 h before the injection of BTAH. To achieve a certain concentration of BTAH, a small volume of a concentrated solution of BTAH in 3.5% NaCl was injected into the electrolyte and stirred rapidly.

3 Results and discussion

Figure 1 is an illustrative example of the results which show the time variation of the changes in the frequency (Δf) of the quartz crystal and of the mass (Δm in μg). The initial decrease in mass and increase in frequency refer to the corrosion of copper (before the injection of BTAH). The corrosion of copper in this medium is a complex process that leads to the formation of soluble and insoluble corrosion products such as $CuCl_2^-$, $CuCl_2$, CuCl, Cu_2O, and $Cu_2(OH)_3Cl$ [50,51]. While the solid corrosion products remain on the surface, the soluble products pass into the electrolyte leading to a decrease in the mass of the metal. The rate of this process can be readily determined from the slope of the linear part of the mass change, i.e.,

$$\textit{corrosion rate} = -\frac{\partial \Delta m}{\partial t} \tag{5}$$

The results in Fig. 1 yield a corrosion rate of about 0.008 μg/s which amounts to 1.26×10^{-10} mol/s (assuming the product is Cu^+). The amount of copper ions that passed into the corrosive medium as a result of the corrosion reaction before injecting BTAH ($\simeq 27$ μg) amounts to about 4.25×10^{-7} mol of Cu^+.

3.1 Injection of BTAH

Upon injection of BTAH in the electrolyte, the trends of Δf and Δm are reversed quite rapidly, indicating an increase in the mass of the copper layer on the quartz crystal. This is attributed to the attachment of BTAH on the copper surface and the formation of the protective Cu(I)BTAH complex [see Equations (1) and (2)]. Had BTAH merely stopped the corrosion reaction, one would have observed a constant mass and constant frequency after the addition of BTAH. Such a behavior has been recently reported on copper in sulfuric acid upon injection of 5-mercapto-1-phenyl tetrazole (5MPhTT), where the mass of copper remained constant for about 10 000 s [48]. The fact that Δm in the present work increased rapidly with time indicates that the corrosion reaction was inhibited and BTAH was attached to the copper surface at a high speed. Three regions can be identified in the course of time variation of Δm and Δf (see Fig. 1).

3.1.1 Region I

Immediately following the addition of BTAH (to establish a concentration of 5×10^{-4} M), there is a rapid linear increase in the mass with time. This is defined as Region I. This region lasts for 130 s (Fig. 1) and is associated with a mass gain of about 6×10^{-6} g which corresponds to 5×10^{-8} mol of BTAH. The protective complex Cu(I)BTA forms readily

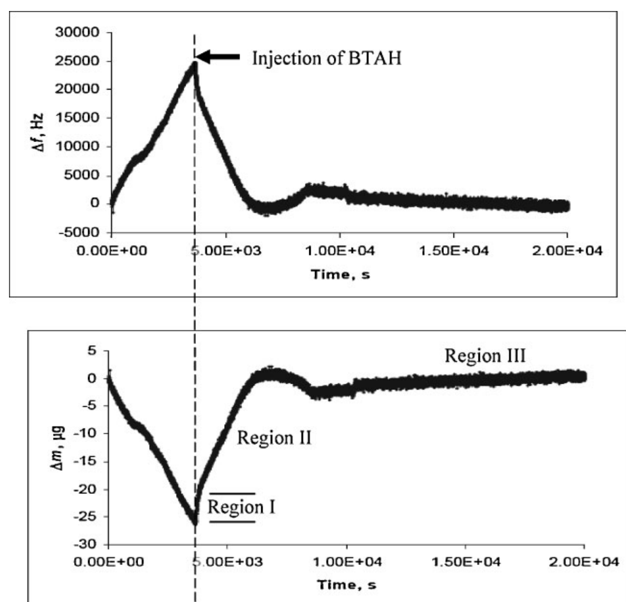

Fig. 1. Changes of resonant frequency and mass of copper in 3.5% NaCl before and after the injection of BTAH into the electrolyte to establish a concentration of 5×10^{-4} M BTAH. The vertical dashed line marks the time of injection of BTAH

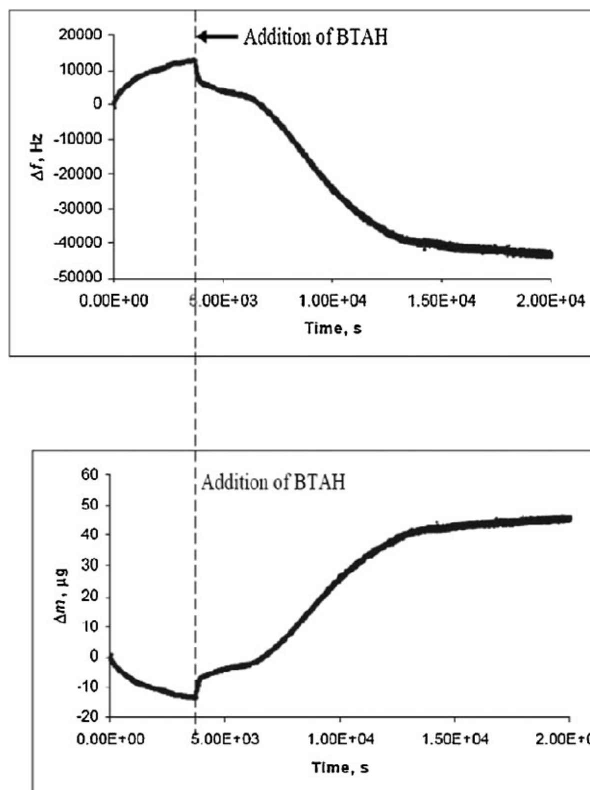

Fig. 2. Changes of resonant frequency and mass of copper in 3.5% NaCl before and after the injection of BTAH into the electrolyte to establish a concentration of 5×10^{-3} M BTAH. The vertical dashed line marks the time of injection of BTAH

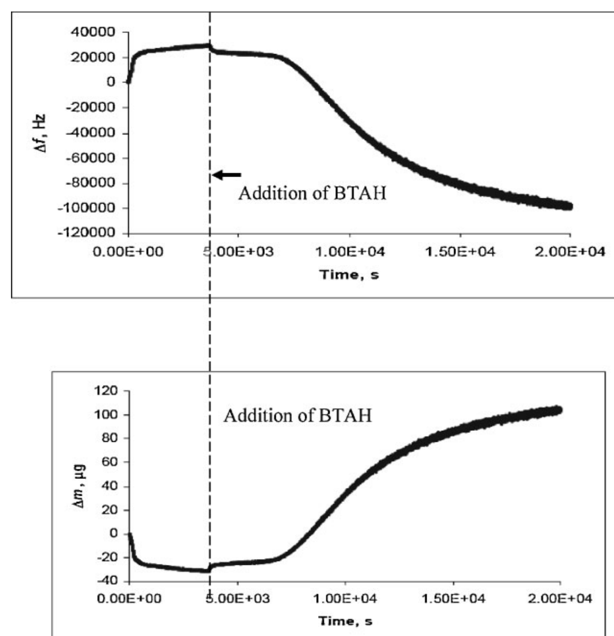

Fig. 3. Changes of resonant frequency and mass of copper in 3.5% NaCl before and after the injection of BTAH into the electrolyte to establish a concentration of 1×10^{-2} M BTAH. The vertical dashed line marks the time of injection of BTAH

the presence of Cu^{+} ions on the surface (e.g., Cu_2O). Since, the Cu^{+} ions are on the metal surface, their reaction with BTAH does not contribute to the mass increase. Hence, the increase in mass is solely attributed to the attachment of BTAH molecules on the surface. The fact that Region I is linear indicates that the rapid attachment of BTAH on the surface and the formation of the Cu(I)BTA complex readily occur on empty sites on the copper surface. The rate of accumulation of BTAH on the surface can be obtained from the slope of the line in Region I. The value of this slope amounts to 4.61×10^{-2} M in Fig. 1 which amounts to 3.87×10^{-10} mol of BTAH adsorbed on the copper surface per second.

The cross-sectional area of a flatly oriented BTAH molecule is estimated at 38.2 Å^2 [13]. Assuming that BTAH accumulates uniformly on the copper surface in a flat orientation, one can readily estimate that at the end of Region I, the protective film of BTAH is about 577 layers thick. Taking the size of a BTAH molecule to be about 0.92 Å [13], the protective film is estimated to be about 530 Å at the end of Region I.

3.1.2 Regions II and III

Region II also shows linear increase in mass with time, at a much lower rate in the presence of 0.5 mM BTAH. The rate of accumulation of BTAH on the surface in Region II amounts to 9.2×10^{-3} μg/s, which is about five-fold slower

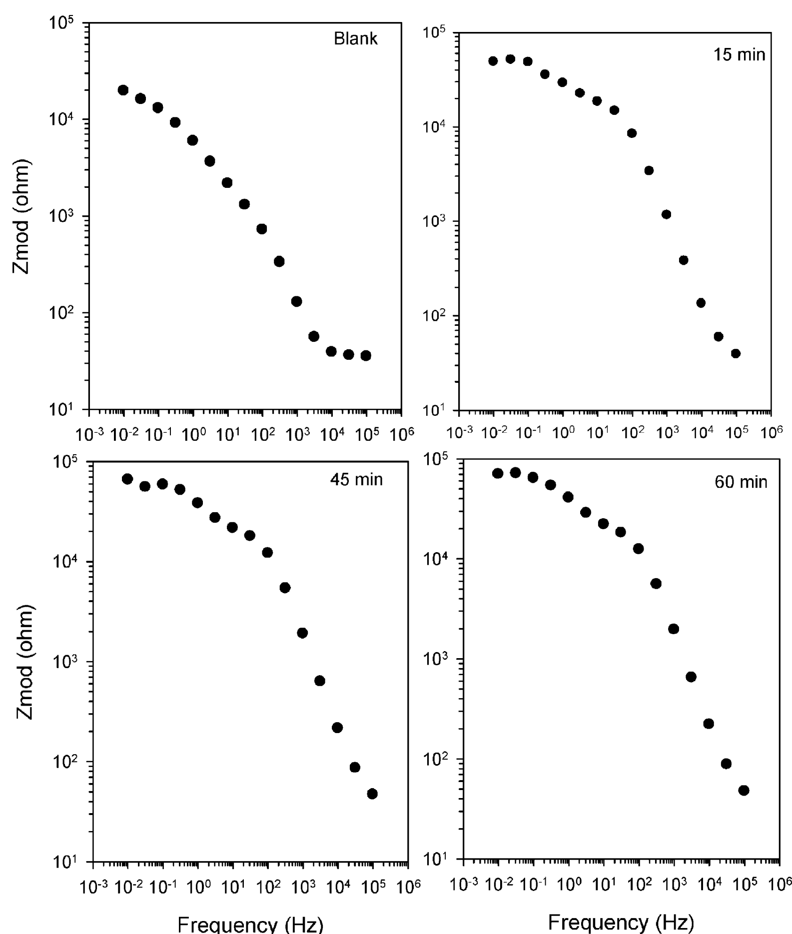

Fig. 4. Bode plots for the electrodeposited copper before (blank) and after various times of injection of BTAH into the electrolyte to achieve a concentration of 5×10^{-3} M BTAH

than in Region I (4.6×10^{-2} μg/s) at the same concentration of BTAH. This region extends for about 40 min which is much longer than Region I. The mass gain during Region II is 20 μg which corresponds to about 1.68×10^{-7} mol of BTAH. This is about three-fold greater than the mass gain in Region I. Region II is attributed to further attachment of BTAH on the surface, albeit at a slower rate. The BTAH that is attached on the surface in Region II is involved in one or both of the following processes:

1- Formation of more of the protective complex Cu(I)BTA, via outward diffusion of Cu^+ ions through the Cu(I)BTA film that formed in Region I.
2- Attachment of BTAH on the Cu(I)BTA film, via physical adsorption, without forming Cu(I)BTAH.

The increase in mass in Region II cannot be readily attributed to the formation of more of the protective Cu(I)BTA complex on the surface. Further growth of the Cu(I)BTA film requires outward diffusion of copper ions through the Cu(I)BTA film (which formed during Region I) to react with BTAH on the surface. In this case, diffusion through the film would be the slow step which requires dependence of mass on the square root of time, i.e., a parabolic rate law. As the film grows linearly with time in Region II, one excludes this possibility. Consequently, Region II is attributed to the attachment of more BTAH on the Cu(I)BTA film that formed during Region I, rather than to the formation of more of the complex Cu(I)BTA.

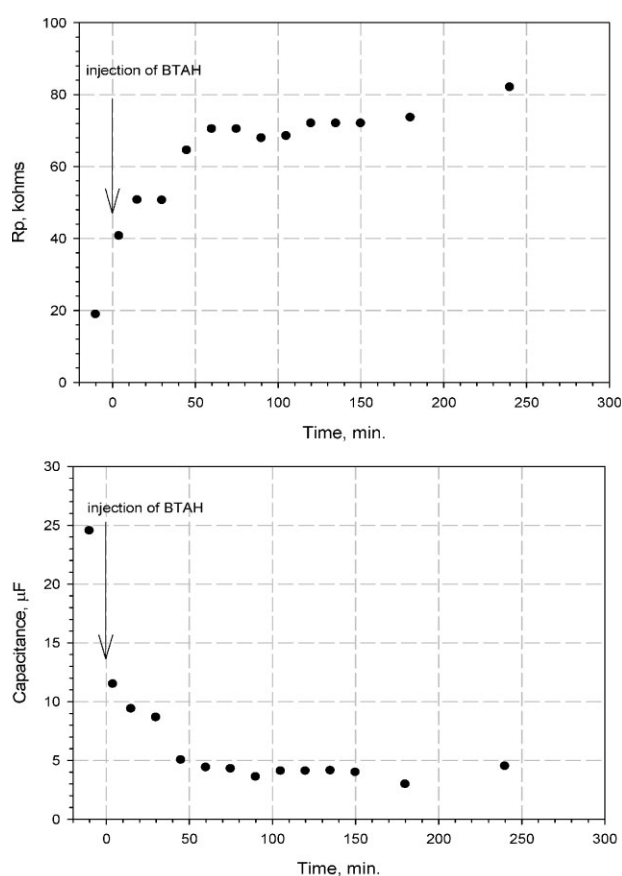

Fig. 5. Variation of the polarization resistance, R_p, and double layer capacity, *C*, for the electrodeposited copper before (blank) and after various times of injection of BTAH into the electrolyte to achieve a concentration of 5×10^{-3} M BTAH

Beyond Region II, the mass remains essentially constant independent of time, indicating that the film has attained its equilibrium thickness under this set of conditions. The film has a limiting mass of 27.4 μg under the conditions of Fig. 1, which corresponds to a thickness of about 0.242 μm (using the arguments presented above).

3.2 Effects of BTAH concentration

The corresponding results in the presence of higher concentrations of BTAH are shown in Figs. 2 and 3 for 5 and 10 mM BTAH, respectively. Region I is seen in all the figures. The mass of BTAH attached to the copper surface during Region I amounts to 6 μg (Figs. 1–3) which is independent of the concentration of BTAH in the electrolyte. It is shown above that this mass is sufficient to form a film of the complex Cu(I)BTA with a thickness of about 530 Å.

As the concentration of BTAH in the electrolyte increases, Region II acquires a sigmoidal shape while the plateau of Region III increases. The complex behavior shown in Region II does not follow the parabolic rate law under any concentration, and hence is not attributed to a diffusional process. The limiting values of Δm at the plateau of Region III are 27.4, 63.4, and 136.3 μg, for 5×10^{-4}, 5×10^{-3}, and 1×10^{-2} M BTAH, respectively. Note that the mass gain of 63.4 μg (plateau in Fig. 2) corresponds to about 5.3×10^{-7} mol of BTAH which is more than all the Cu^+ ions that resulted from the corrosion reaction before injecting BTAH. Since only a fraction of these Cu^+ ions remain on the copper surface during free corrosion, it follows that the amount of BTAH attached to the surface in Region II is much more than what is needed to form the complex Cu(I)BTAH. Coupled with the linear increase in mass with time, this suggests that BTAH adsorbs on the Cu(I)BTA film that formed in Region I.

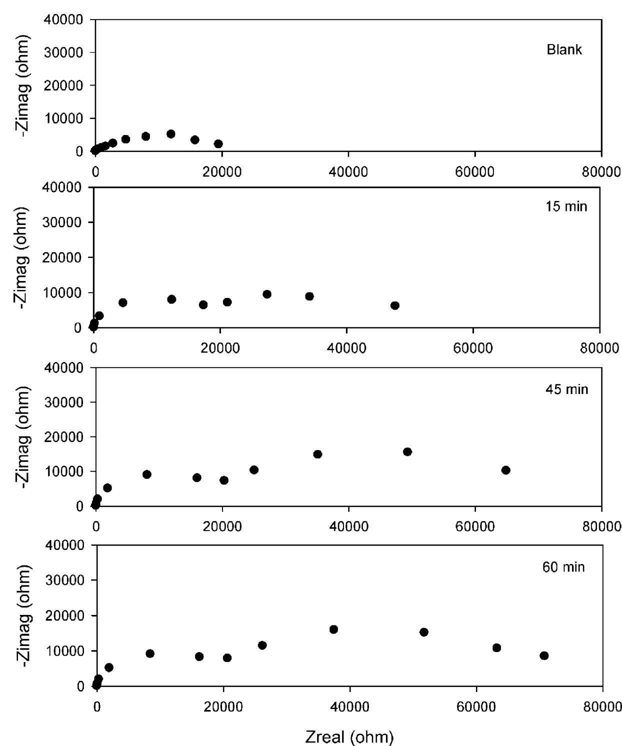

Fig. 6. Nyquist plots for the electrodeposited copper before (blank) and after various times of injection of BTAH into the electrolyte to achieve a concentration of 5×10^{-3} M BTAH

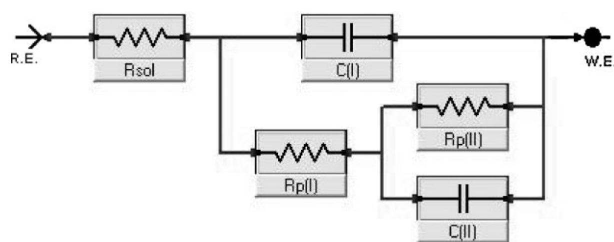

Fig. 7. Illustration of the equivalent circuit that simulates the behavior of the system at various times after the injection of BTAH. R_{sol} refers to the solution resistance, R_p(I) and C(I) refer, respectively to the polarization resistance and double layer capacity of the inner Cu(I)BTA film while R_p(II) and C(II) refer to the corresponding values for the adsorbed BTAH film formed during Region II

Using the argument presented above, the total thickness of the film amounts to 0.053, 0.123, and 0.264 μg at 5×10^{-4}, 5×10^{-3}, and 10^{-2} M BTAH, respectively.

3.3 Electrochemical impedance spectroscopy

Electrochemical impedance spectra were measured on the electrodeposited copper in the absence of BTAH and at various times after injecting BTAH. Some of the results are illustrated in Fig. 4 in the form of Bode plots. The impedance of the interface Z_{mod} includes real (Z_{real}) and imaginary (Z_{imag}) components. It depends on the resistance of the solution between the reference electrode and the surface of the test electrode (R_{sol}), the polarization resistance, R_p, which measures the resistance of the interface to change transfer, the frequency of the signal (f), and the double layer capacity C. There are two important limiting values of the total impedance of the circuit, Z_{mod}, in the Bode plot (Fig. 4). The first is obtained at a very high frequency where $Z \simeq R_{sol}$, i.e., the impedance of the circuit is primarily caused by the resistance of the solution. The second limiting value is obtained at very low frequencies where the total impedance of the circuit is the sum of R_p and R_{sol}, i.e., $Z \simeq R_p + R_{sol}$. Consequently, both R_{sol} and R_p can be obtained from the values of the limits of Z_{mod} at the right- and left-hand sides of the Bode plot. Both values and the double layer capacity can also be obtained by fitting the impedance spectrum to the behavior of an equivalent circuit (as discussed below). Figure 4 reveals that the sum $R_p + R_{sol}$ is about three orders of magnitude greater than R_{sol}. Consequently the low frequency limit is taken to be R_p. It is also clear that R_p increases with the time of contact of BTAH with the surface.

Figures 5a and b display, respectively, the effect of time on the polarization resistance and the double layer capacity of the interface. Note the rapid increase in R_p and rapid decrease in C at short time. This corresponds to Region I during which the film of Cu(I)BTAH forms rapidly upon the attachment of BTAH to the surface. Beyond this initial rapid increase, R_p increases more gradually with time toward a plateau. The behavior is quite similar to that shown in Figs. 1 and 2.

Figure 6 shows a series of Nyquist plots obtained before and at various times of injection of BTAH into the electrolyte. The Nyquist plot of the blank electrolyte shows one time constant with a polarization resistance $R_p \simeq 20\,\text{k}\Omega$. On the other hand, two time constants appear in the Nyquist plots after injecting BTAH. It is also interesting to note that the magnitude of the impedance corresponding to the second

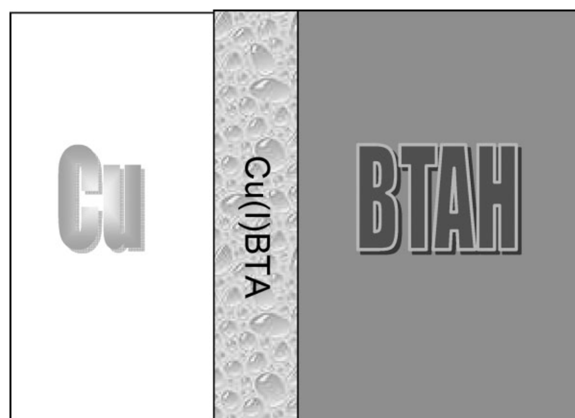

Fig. 8. Schematic illustration of the inner layer of Cu(I)BTA complex that forms in Region I and the outer layer of BTAH adsorbed during Region II on the Cu(I)BTA. The outer layer grows in mass and thickness with time

time constant increases with the time of contact of BTAH with the electrode, while that corresponding to the first time constant remains constant. The measured EIS spectra were satisfactorily fitted to the equivalent circuit shown in Fig. 7. The circuit simulates the impedance response of a heterogeneous surface with two distinct pairs of R and C values connected in parallel (two time constants).

4 Conclusions

The interaction of BTAH with the surface of corroding copper is described in terms of two time-dependent Regions I and II, before reaching equilibrium. Region I shows the linear growth of the Cu(I)BTA complex with time. The thickness of the film that forms at the end of region I amounts to 530 Å, independent of the concentration of BTAH in the electrolyte. Region II shows further attachment of BTAH on the surface to reach a plateau (Region III) indicating the attainment of an equilibrium thickness of the film. As the concentration of BTAH increases, the shape of Region II changes and the value of the plateau (Region III) increases, indicating a thicker film of BTAH under equilibrium condition. While Region I is attributed to the formation of the complex Cu(I)BTA, Region II is attributed to the adsorption of BTAH on the Cu(I)BTA, rather than the formation of more Cu(I)BTA (Fig. 8). The growth of both regions is associated with the increase in the polarization resistance and decrease in the double layer capacity. The impedance spectra reveal two time constants which are well correlated to Regions I and II.

Acknowledgements: The authors gratefully acknowledge the support of this work by the Research Administration of Kuwait University, under Grant Number SC03/02.

5 References

[1] T. Hashemi, C. A. Hogarth, *Electrochim. Acta* **1988**, *33*, 1123.
[2] P. G. Fox, G. Lewis, P. J. Boden, *Corros. Sci.* **1979**, *19*, 457.
[3] J. B. Cotton, I. R. Scholes, *Br. Corros. J., Lond.* **1967**, *2*, 1.

[4] F. El-Taib Haekal, S. Haruyama, *Corros. Sci.* **1980**, *20*, 887.
[5] H. Y. H. Chan, M. J. Weaver, *Langmuir* **1999**, *15*, 3348.
[6] W. Polewska, M. R. Vogt, O. M. Magnussen, R. J. Behm, *J. Phys. Chem. B* **1999**, *103*, 10440.
[7] D. Tromans, G. Li, *Electrochem. Solid State* **2002**, *5*, 5.
[8] Z. D. Schultz, M. E. Biggin, J. O. White, A. A. Gewirth, *Anal. Chem.* **2004**, *76*, 604.
[9] A. T. Al-Hinai, K. Osseo-Asare, *Electrochem. Solid State* **2003**, *6*, 23.
[10] S. Hegde, S. V. Babu, *Electrochem. Solid State* **2003**, *6*, 126.
[11] T.-H. Tsai, S.-C. Yen, *Appl. Surf. Sci.* **2003**, *210*, 190.
[12] B. D. Vogt, E. K. Lin, W.-L. Wu, C. C. White, *J. Phys. Chem. B* **2004**, *108*, 12685.
[13] A. Frignani, M. Fonsati, C. Monticelli, G. Brunoro, *Corros. Sci.* **1999**, *41*, 1217.
[14] C. Jin-Hua, L. Zhi-Cheng, C. Shu, N. Li-Hua, Y. Shou-Zhuo, *Electrochim. Acta* **1997**, *43*, 265.
[15] J. Telegdi, A. Shaban, E. Kalman, *Electrochim. Acta* **2000**, *45*, 3639.
[16] M. Metikos-Hukovic, R. Babic, A. Marinovic, *J. Electrochem. Soc.* **1998**, *145*, 4045.
[17] R. Ravichandran, N. Rajendran, *Appl. Surf. Sci.* **2005**, *239*, 182.
[18] R. Ravichandran, S. Nanjundan, N. Rajendran, *J. Appl. Electrochem.* **2004**, *34*, 1171.
[19] D. Papapanayiotou, H. Deligianni, R. C. Alkire, *J. Electrochem. Soc.* **1998**, *145*, 3016.
[20] N. Tantavichet, M. Britzker, *J. Appl. Electrochem.* **2006**, *36*, 49.
[21] S. Mieczyslaw, J. Malyszko, *J. Electrochem. Soc.* **2000**, *147*, 1758.
[22] W. Schmidt, R. C. Alkire, A. A. Gewirth, *J. Electrochem. Soc.* **1996**, *143*, 3122.
[23] S. Deshpande, S. C. Kuiry, M. Klimov, Y. Obeng, S. Seal, *J. Electrochem. Soc.* **2004**, *151*, G788;
[23a] S. Deshpande, S. C. Kuiry, M. Klimov, S. Seal, *J. Electrochem. Solid State* **2005**, *8*, G98.
[24] X. J. Li, D. M. Guo, R. K. Ren, Z. J. Jin, *Key Engineering Materials*, **2006**, *304–305*, 350.
[25] J.-Y. Fang, M. S. Tsai, B. T. Dai, S. Y. Wu, M. S. Feng, *Electrochem. Solid-State Lett.* **2005**, *8*, G128.
[26] K. Babic-Samardzija, N. Hackerman, *J. Solid. State Electrochem.* **2005**, *9*, 483.
[27] S. Y. Sayed, M. S. El-Deab, B. E. El-Anadouli, B. G. Ateya, *J. Phys. Chem. B* **2003**; *107*, 5575.
[28] P. G. Gao, J. L. Yao, J. W. Zheng, R. A. Gu, Z. Q. Tian, *Langmuir* **2002**, *18*, 100.
[29] V. Brusic, M. A. Frisch, B. N. Eldredge, F. P. Novak, F. B. Kanfman, B. M. Rush, G. S. Frankel, *J. Electrochem. Soc.* **1991**, *138* 2253.
[30] A. M. Fenelon, C. B. Breslin, *J. Appl. Electrochem.* **2001**, *31*, 509.
[31] R. Walker, *Br. Corros. J.* **1999**, *34*, 304.
[32] J. F. Walsh, H. S. Dhariwal, A. Gutierrez-Sosa, P. Finetti, C. A. Muryn, N. B. Brookes, R. J. Oldman, G. Thornton, *Surf. Sci.* **1998**, *415*, 423.
[33] Y. Jiang, J. B. Adams, D. Sun, *J. Phys. Chem. B* **2004**, *108*, 12851.
[34] H. S. Hegazy, E. A. Ashour, B. G. Ateya, *J. Appl. Electrochem.* **2001**, *31*, 1261.
[35] G. W. Poling, *Corros. Sci.* **1970**, *10*, 359.
[36] F. Mansfield, T. Smith, E. T. Parry, *Corrosion* **1971**, *27*, 289.
[37] C. Clerc, R. Alkire, *J. Electrochem. Soc.* **1991**, *138*, 25.
[38] R. Alkire, A. Cangellari, *J. Electrochem. Soc.* **1989**, *136*, 913.
[39] G. Sauerbrey, *Z. Phys.* **1959**, *155*, 206.
[40] K. A. Marx, *Biomacromolecules* **2003**, *4*, 1099.
[41] B. D. Vogt, E. K. Lin, W.-L. Wu, C. C. White, *J. Phys. Chem. B* **2004**, *108*, 12685.
[42] A. Zhou, B. Xie, N. Xie, *Corros. Sci.* **2000**, *42*, 469.
[43] K. Mansikkamaki, P. Ahonen, G. Fabricius, L. Murtomaki, K. Kontturi, *J. Electrochem. Soc.* **2005**, *152*, B12.
[44] W. Qafsaoui, C. Blanc, N. Pebere, H. Takenouti, A. Srhiri, G. Mankowski, *Electrochim. Acta* **2002**, *47*, 4339.
[45] M. Hepel, E. Cateforis, *Electrochimica Acta* **2001**, *46*, 3801.
[46] M. Fonsati, F. Zucchi, G. Trabanelli, *Electrochim. Acta* **1998**, *44*, 331.
[47] P. Kern, D. Landolt, *J. Electrochem. Soc.* **2001**, *148*, B228.
[48] E. Szocs, Gy. Vastag, A. Shaban, E. Kalman, *Corros. Sci.* **2005**, *47*, 893.
[49] K. Mansikkamaki, P. Ahonen, G. Fabricius, L. Murtomaki, K. Kontturi, *J. Electrochem. Soc.* **2005**, *152*, B12.
[50] M. Chmielova, J. Seidlerova, Z. Weiss, *Corros. Sci.* **2003**, *45*, 883.
[51] G. Kear, B. D. Barker, F. C. Walsh, *Corros. Sci.* **2004**, *46*, 109.

(Received: May 8, 2007) W4104
(Accepted: June 25, 2007)